Schwarz and Blower, http://www.jcb.org/cgi/content/full/jcb.201406037/DC1

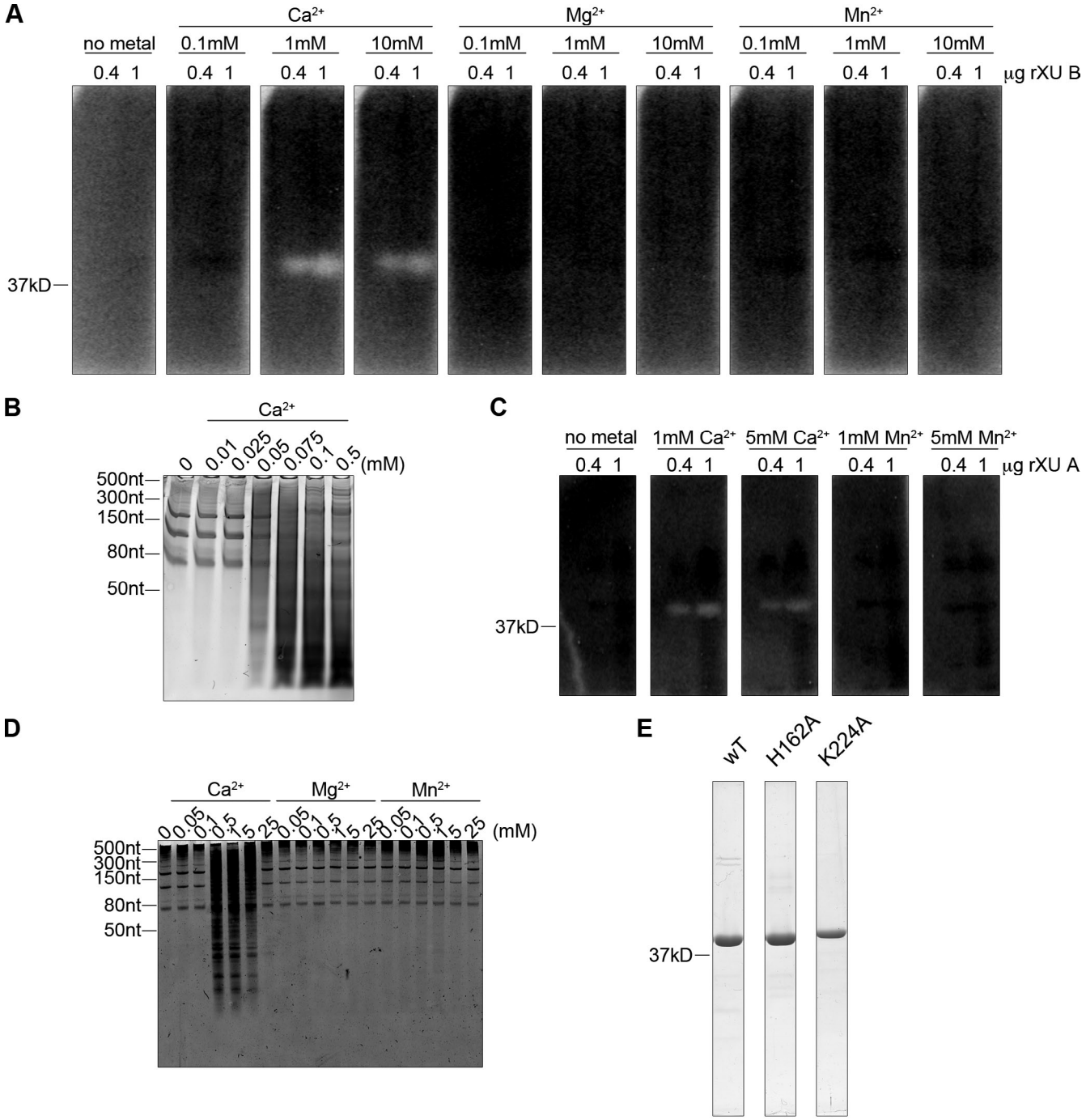

Figure S1. **In vitro characterization of recombinant XendoU.** (A) Recombinant XendoU B was subjected to an in-gel nuclease assay. Either 0.4 or 1 µg of purified XendoU B was electrophoresed through an SDS-PAGE gel that contained radiolabeled mRNA. Gels were soaked in buffer to remove SDS and renature proteins, then incubated in buffers containing no metal or increasing concentrations of $CaCl_2$, $MgCl_2$, or $MnCl_2$. Gels were exposed to a PhosphorImager plate and scanned on the Typhoon TRIO. (B) Recombinant XendoU B (0.05 µM) was incubated with total RNA from CSF and buffers containing no metal or increasing concentrations of $CaCl_2$ as in Fig. 2 A but with a finer calcium gradient to determine the minimal calcium required for activation. RNAs were run on a denaturing acrylamide gel and stained with SYBR Green II. (C) Recombinant XendoU A was subjected to an in-gel nuclease assay as described in A in the presence of $CaCl_2$ and $MnCl_2$. (D) Recombinant XendoU A (0.05 µM) was incubated with total RNA from CSF and buffers containing no metal or increasing concentrations of $CaCl_2$, $MgCl_2$, or $MnCl_2$ (as described for XendoU B; Fig. 2 A). RNAs were run on a denaturing acrylamide gel and stained with SYBR Green II. (E) Coomassie-stained SDS-PAGE gel of 6×His purified recombinant XendoU B wT, H162A, and K224A proteins.

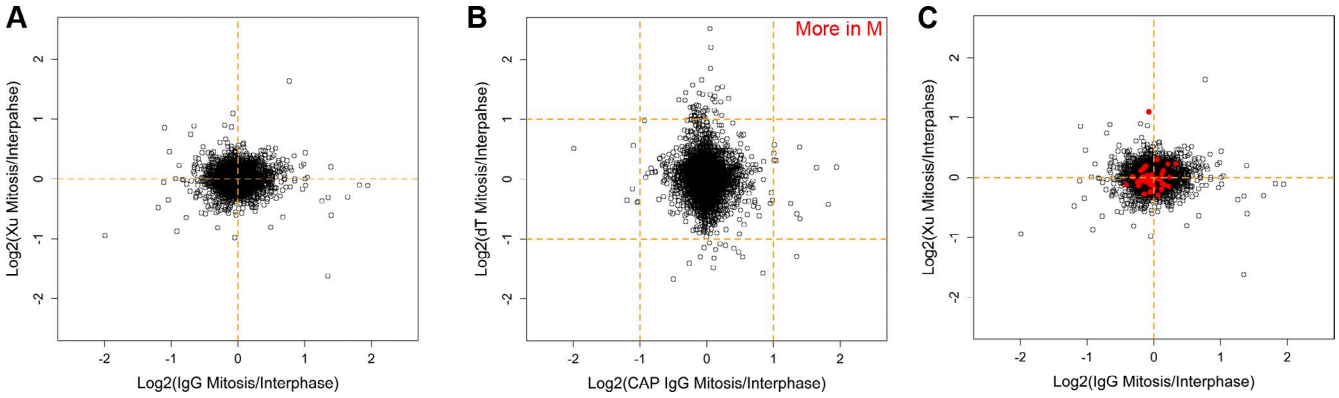

Figure S2. **Analysis of RNA stability at meiosis to interphase transition in *X. laevis* egg extracts.** (A) mRNAs were purified from CSF-arrested or interphase (0.6 mM $CaCl_2$) control-depleted (rabbit IgG) or XendoU-depleted extracts using CAP-capture. mRNAs were sequenced on an Illumina sequencer and aligned to gene models in the draft *X. laevis* genome (7.0 downloaded from Xenbase). The ratio (CSF/Interphase [M/IF]) of each mRNA with >100 total reads in CSF and interphase extracts for each condition is plotted. Few mRNAs exhibit a twofold change in apparent abundance in control extracts but not in XendoU-depleted extracts. (B) mRNA was purified from CSF and interphase (0.6 mM $CaCl_2$) extracts using oligo dT as the selection. The ratio of each mRNA between mitosis and interphase in CAP-captured mRNAs is compared with those in dT-purified mRNAs. mRNAs purified by dT selection exhibit more apparent variation due to changes in poly-A tail length. In addition, there are no mRNAs that exhibit a twofold change in abundance in both dT and CAP-capture purified mRNAs (upper right quadrant). (C) Same plot as in A, with mRNAs that exhibit a twofold change (M/IF) in dT-selected mRNAs highlighted in red. This graph demonstrates that there are no mRNAs that exhibit major degradation at the M-to-IF transition in a XendoU-dependent manner.

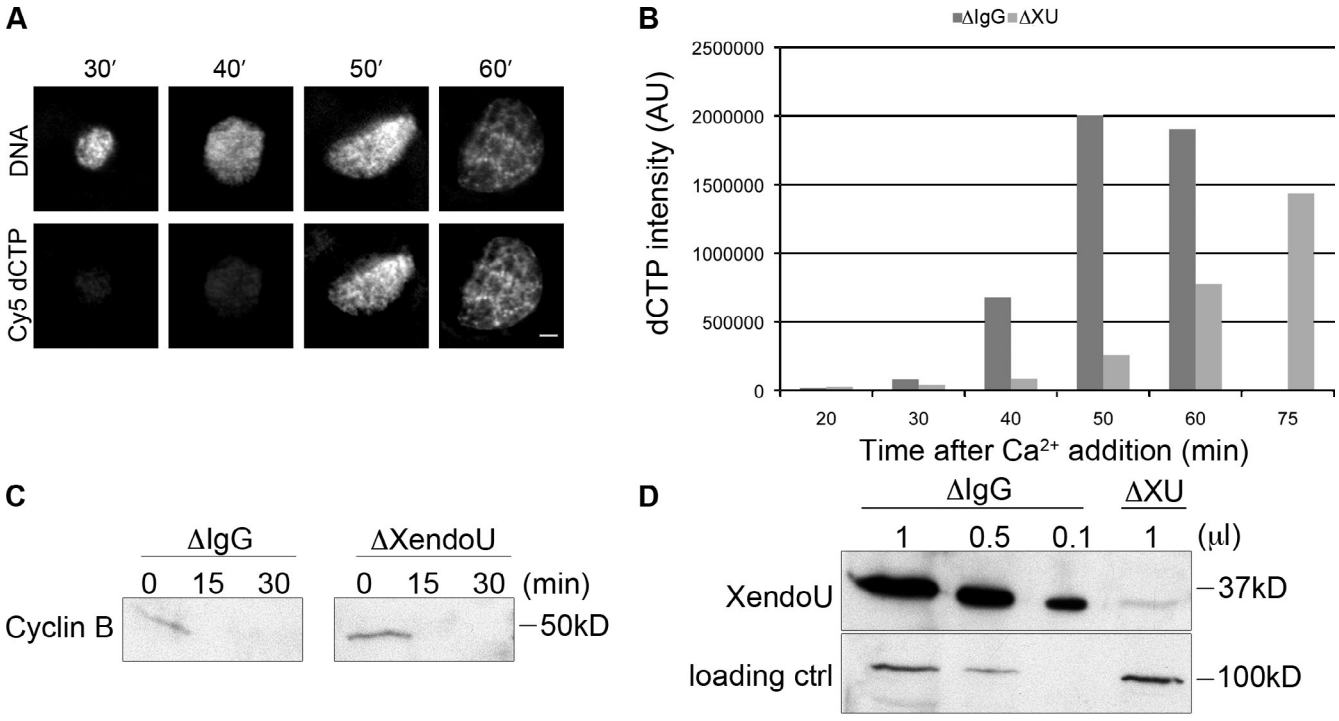

Figure S3. **XendoU is involved in proper timing of DNA replication.** (A) Demembranated *X. laevis* sperm nuclei were incubated in CSF extract in the presence of 0.6 mM $CaCl_2$ and Cy5-labeled dCTP. Aliquots of the reactions were taken at the time points indicated, mixed with DAPI, and imaged for DNA (total DNA [DAPI] or newly synthesized DNA [Cy5]). Replication (Cy5 incorporation) begins at 40 min after calcium addition. Bar, 10 μm. (B) CSF was either mock-depleted (IgG) or XendoU-depleted and mixed with Cy5 dCTP as in A. Aliquots were taken every 10 min after $CaCl_2$ addition, and mean intensity of Cy5 was measured. XendoU-depleted extracts demonstrated a severe delay in the start of replication. The data presented are from a single representative experiment that was performed four times. (C) CSF extract was depleted as in B. Proteins were isolated from time points taken every 15 min after calcium addition and blotted for cyclin B. Cyclin B degradation was unaffected in XendoU-depleted extracts. (D) Western blot demonstrating completion of depletion in XendoU supernatants after immunodepletion of CSF with protein A Dynabeads bound with XendoU antibody. The loading control is importin β.

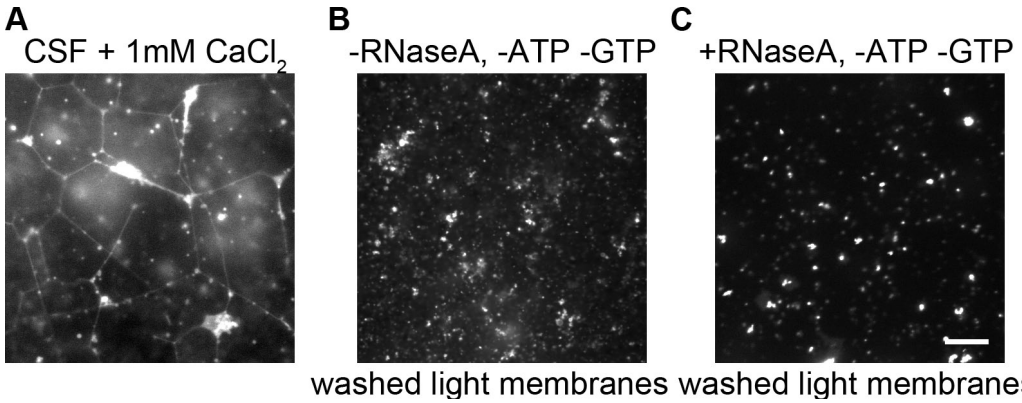

Figure S4. **CSF ER network formation and –ATP –GTP vesicle fusion controls.** (A) CSF extract was incubated in the presence of 1 mM $CaCl_2$ for 60 min followed by staining of membranes by octadecyl rhodamine and imaged live as in Fig. 3 (B and C) to demonstrate improved network formation in extracts that are not incubated with Dynabeads. (B) Vesicle fusion control reactions (−ATP –GTP) of wlms in the absence of RNase A treatment (as in Fig. 5 F) to show the absence of ER tubules. (C) Vesicle fusion control reactions as in B of wlms treated with 0.1 ng/µl RNase A to show the absence of ER tubule formation. Bar, 10 µm.

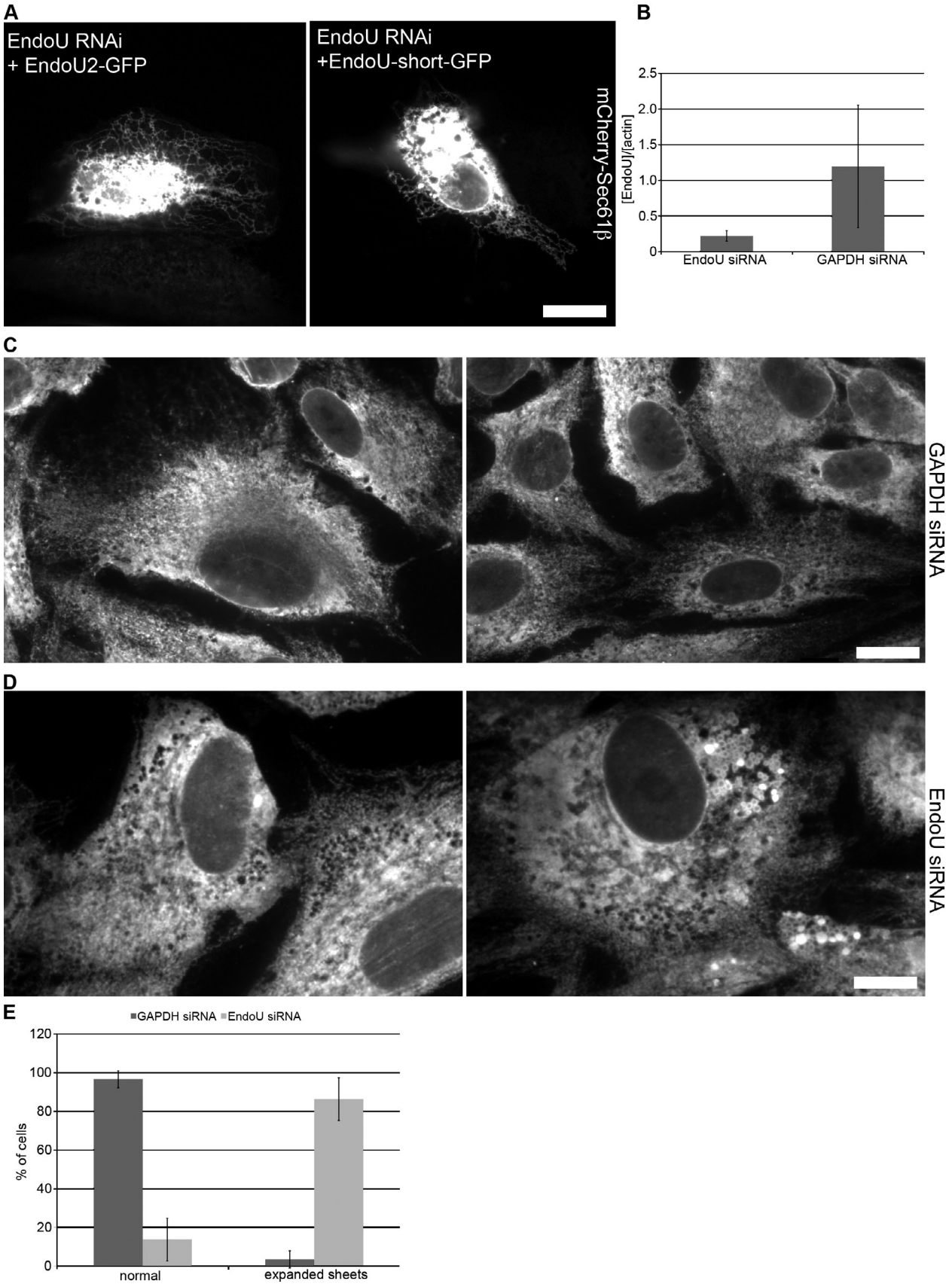

Figure S5. **EndoU siRNA knockdown.** (A) HeLa cells incubated with esiRNAs against the 3′ UTR of EndoU exhibit rescue phenotypes (as graphed in Fig. 6 G) when transfected with EndoU2-GFP or EndoU-short-GFP constructs (resistant to RNAi, lacking the 3′ UTR). ER is visualized with mCherry-Sec61β. (B) Expression of EndoU was reduced in HeLa cells using siRNAs. RNA from control and siRNA cell populations was collected and analyzed by quantitative RT-PCR for EndoU and actin. EndoU expression is normalized to actin expression in each sample. Expression levels were monitored in three experiments. Error bars indicate standard deviation. (C) ER morphology in control cells stained with anti-kinectin antibodies. (D) ER morphology in EndoU siRNA cells stained with anti-kinectin antibodies. (E) Quantification of normal and expanded ER sheets in control and EndoU RNAi cells. At least 200 cells were scored from three experiments for each condition. Error bars indicate standard deviation. Bars, 10 µm.

Supplemental script S1, uniquefastq.pl, is a Perl script that collapses all the reads in a fastq file into unique reads.

Supplemental script S2, removerrna.pl is a Perl script that uses the SAM alignment file of reads aligned against rRNA to remove these reads from a fastq file.

Both are available as a ZIP file.